Asian Journal of Chemistry; Vol. 35, No. 5 (2023), 1189-1198

ASIAN JOURNAL OF CHEMISTRY

https://doi.org/10.14233/ajchem.2023.27805

Investigation of Guanidine-Curcumin Complex based on Quantum Chemicals, Pharmacokinetics and Molecular Docking Simulation against Breast Cancer: A Theoretical Approach

THIMMA MOHAN VISWANATHAN[1], AZAR ZOCHEDH[1], KALIRAJ CHANDRAN[1], SUREBA SUKUMARAN[1], ASATH BAHADUR SULTAN[2,*] and THANDAVARAYAN KATHIRESAN[1,*]

[1]Department of Biotechnology, Kalasalingam Academy of Research and Education, Krishnankoil-626126, India
[2]Condensed Matter Physics Laboratory, Department of Physics, International Research Centre, Kalasalingam Academy of Research and Education, Krishnankoil-626126, India

*Corresponding author: E-mail: s.asathbahadur@gmail.com; t.kathiresan@klu.ac.in

Received: 29 March 2023; *Accepted*: 12 April 2023; *Published online*: 28 April 2023; AJC-21228

The breast cancer is the foremost reason for cancer death rates and incidence globally in women. Combinatorial therapy is a significant practice in the cancer treatment process. The combination of two molecules appears efficient and inhibits a variety of cancer-causing mechanisms. In present investigation, combination of guanidine and curcumin was employed as a synergistic drug against the breast cancer. Firstly, the combined structure of guanidine-curcumin was built and the structure was optimized through density functional computation in B3LYP/6-311++G (d,p) level. The electronic spectrum observed in CAM-B3LYP with same basis set and the transition observed was $\pi \rightarrow \pi^*$. The chemical reactivity and structural stability of guanidine-curcumin was evaluated through molecular orbitals and molecular electrostatic potential. The energy gap calculated for the complex structure was 3.45963 eV, which confirms the better reactivity of the complex. The atomic charges of each atom associated with the complex was assessed through Mulliken charge distribution. Further, the breast cancer inhibitory potential of guanidine-curcumin complex was evaluated through *in silico* molecular docking studies. The docking simulation showed that the complex structure has good binding ability against target breast tumor proteins when compared with standard drug. The physico-chemical, absorption, metabolism, distribution, excretion and toxicity characteristics of complex structure exhibited the drug-likeness properties and showed its safety feature. These, *in silico* findings will be beneficial for further *in vitro* and *in vivo* studies against breast cancer.

Keywords: Guanidine, Curcumin, Breast cancer, Density function theory, ADMET.

INTRODUCTION

Breast cancer is the primary reason of cancer mortality and incidence among women worldwide. As reported by the ICMR, India constantly reported 144,000 new instances of breast cancer and placed third in cancer rates with a proportion of 68.4% fatalities per year. Moreover, roughly 30% of people continue to live after being diagnosed with breast cancer for five years [1]. Guanine oxidation produces guanidine, a crystalline substance with a high alkalinity. It is a crucial molecule with a "CN3" core that has a variety of unique features. Guanidine molecules are extremely important chemically and biologically and their hydrophilic character significantly contributes to the stability of protein conformations through hydrogen bonding. The primary guanidine functions were widely distributed in natural goods and pharmaceutically active substances [2]. The important active ingredient of the dietary spice turmeric, curcumin (diferuloylmethane) is a naturally occurring phenolic molecule derived from the plant *Curcuma longa*. Curcumin is a highly pleiotropic chemical that may mediate chemotherapy and chemopreventive effects on cancer through a variety of pathways while being safe and having minimal to no side effects [3]. Combinatorial treatment is a widespread technique in the treatment of cancer. The combination of two lead molecules is an effective and targets various mechanism of cancer. Chemotherapy for breast cancer is defined by directing on the mechanism of target receptors such as progesterone receptor (PR), estrogen receptor (ER) and epidermal growth factor receptor (EGFR). The development and metastasis of breast cancer are significantly influenced by the oestrogen receptor. Several studies demonstrated

that oestrogen, namely 17b-estradiol, increases *c*-Myc and cyclin D1 synthesis and activity, resulting in the transition of epithelial cells of the mammary organ from G1 phase to S phase of the cell cycle. An alternative to oestrogen therapy is a potential treatment for ER-positive breast cancer [4]. The overexpression of PR is often seen in malignancy and is immediately seen by the excess expression of ER. It is the outcome of estrogenic stimulation in tumour locations that displayed a functional ER pathway. When PR and ER are overexpressed jointly, there are higher chances of responding to hormone therapy and a better prognosis for the development of PR positive breast tumours [5]. The administration of ER and PR antagonists may lead to a better prognosis and therapeutic management. EGFR is said to be a key factor in triple-negative breast cancer (TNBC) [6]. The therapy choices are extremely restricted for TNBC since it is phenotypically characterized as being ER, PR and HER-2 negative [7]. Because of this, using EGFR intermediate antagonists can offer effective treatment strategies. Earlier study demonstrated that the tumor-associated macrophages (TAMs) create the chemokine ligand 18 (CCL18), that is regarded to be a viable therapeutic focus, to promote the progression of breast cancer [8]. The BCL-2 protein family, which is essential for regulating cell death, changes the inner mitochondrial membranes to cause apoptosis [9]. Breast cancer metastatic routes are associated with cell cycle drivers, transcriptional factors and oncogenic proteins like tyrosine kinase. These proteins and HSP90 interact and it has been proposed that blocking HSP90 might be a viable treatment for breast cancer [10].

Although computational molecular modelling is a useful technique for looking at a variety of particles and nanostructures, it is most useful for locating compounds and verifying their structural relationships. In present evaluation, constructed guanidine curcumin complex was studied as a potential therapeutic target using a combination of molecular docking simulation and density function theory designs. Density functional theory (DFT) with B3LYP/6-311++G (d,p) basis set was used to evaluate the molecular geometry, structural stability, molecular reactivity, mulliken atomic charge distribution and molecular electrostatic potential analysis of the complex structure [11]. Then, the *in silico* molecular docking studies was done to estimate the binding ability of the constructed complex structure against the breast cancer associated target proteins. The physico-chemical and ADMET characteristics of the guanidine-curcumin was evaluated to assess the drug-likeness profile of the complex structure. These *in silico* findings will be helpful for further *in vitro* and *in vivo* investigations in breast cancer.

EXPERIMENTAL

Construction of complex structure: The guanidine and curcumin complex were constructed using ChemDraw tool. Initially, guanidine and curcumin structures were retrieved from PubChem (https://pubchem.ncbi.nlm.nih.gov/) online database in ".sdf" format. The combination of two structure and their reactive binding sites was confirmed through ChemDraw Pro tool. The constructed complex structure was saved in ".sdf" format and was utilized for further studies.

Quantum chemical calculations: The electrical action of guanidine carbonate and curcumin complex was essential to its pharmacological effectiveness. In terms of three-dimensional electronic density system, DFT is a useful theory for determining the electronic states of atoms, molecules and solids [12]. The Gaussian 09W programme and the GaussView molecular visualization tools were used for quantum computational investigation of the title compound. The molecular structure of guanidine carbonate and curcumin complex was optimized using the DFT/Becke-3-Lee-Yang-Parr (B3LYP) method having a 6-311++G (d, p) basis set [13]. Then, from the optimized complex structure bond angles and bond length were analyzed. Electronic transitions were observed by theoretical UV-visible spectrum. The frontier molecular analysis, Mulliken charge distribution and molecular electrostatic potential analysis of the complex structure which were analyzed in the same basis set and were visualized using the molecular visualization tool GaussView 5.

Retrieval and processing of target proteins: The three-dimensional structure of targeted breast cancer associated receptor proteins was saved from the database of RCSB Protein Data Bank (PDB) (https://www.rcsb.org/) [14]. The ".pdb" formatted breast cancer proteins were BCL2, CCL18, EGFR, ERα, PR, HER-2 and HSP90 with the PDB IDs 4AQ3, 4MHE, 2J6M, 6WOK, 4OAR, 2IOK and 2VCJ, respectively. Then, the BIOVIA Discovery studio tool was used to adding requisite and removing of other ligands, hetatms and water molecules in the prepared protein structure.

Molecular docking: Molecular docking was done for all the seven target breast cancer associated proteins with guanidine and curcumin complex along with a standard molecule through PyRx 0.8 software [15]. The optimized constructed complex structure was then evaluated for binding efficiency against target proteins. The complex structure was first imported into PyRx workspace followed up by the loading of target proteins. Then the grid box was constructed at the ideal binding regions and then the docking was performed. Further, the output of the docking was investigated through BIOVIA discovery studio for analyzing bond category, distance of each bond formed and for visualization of interactions.

Pharmacokinetics study: The physio-chemical, ADME and toxicity profiles of guanidine-curcumin complex were analyzed *via* the SwissADME (http://www.swissadme.ch/) and pkCSM online tool (http://biosig.unime.edu.au/pkcsm/prediction) [16]. The canonical SMILES of complex structure derived from ChemDraw tool. These SMILES file was then utilized as an input for SwissADME and pkCSM analysis.

RESULTS AND DISCUSSION

Molecular geometry: The structure of guanidine-curcumin complex was optimized for the analysis of molecular geometry of the constructed system. The optimization was computed through B3LYP/6-311++G (d,p) level and further, bond length and bond angles in the structure were studied. The optimized structure of guanidine-curcumin (Fig. 1) and the values of bond length and bond angles are shown in Table-1. The structure

TABLE-1
BOND LENGTH (Å) AND BOND ANGLE (°) OF CONSTRUCTED GUANIDINE-CURCUMIN COMPLEX

Atoms	Bond length (Å)	Atoms	Bond length (Å)	Atoms	Bond length (Å)	Atoms	Bond length (Å)
O1-C12	1.3955	C8-C17	1.4581	C22-H36	1.0837	C12-C18	1.4157
O1-C26	1.4499	C9-C20	1.5283	C23-H37	1.0870	C13-C19	1.4127
O2-C13	1.3848	C9-C21	1.5360	C24-H38	1.0855	C14-C22	1.3915
O2-C27	1.4515	C9-H28	1.0961	C25-H39	1.0852	C14-H32	1.0841
O3-C18	1.3602	C15-C23	1.3948	C26-H42	1.0964	N50-C51	1.2949
O3-H40	1.0359	C15-H33	1.0836	C26-H43	1.0961	C27-H47	1.0891
O4-C19	1.3836	C16-C24	1.3582	C26-H44	1.0896	H44-H54	5.9161
O4-H41	0.9769	C16-H34	1.0902	C27-H45	1.0966	N48-C51	1.3478
O5-C20	1.2570	C17-C25	1.3548	C27-H46	1.0966	N48-H52	1.0152
O6-C21	1.2515	C17-H35	1.0900	C9-H29	1.0919	N48-H53	1.0087
C7-C10	1.4176	C18-C22	1.4020	C10-C12	1.3886	N49-C51	1.4628
C7-C14	1.4113	C19-C23	1.3974	C10-H30	1.0842	N49-H54	1.0256
C7-C16	1.4528	C20-C24	1.4640	C11-C13	1.3923	N49-C55	1.3239
C8-C11	1.4160	C21-C25	1.4687	C11-H31	1.0842	N50-H56	1.0168
C8-C15	1.4077	–	–	–	–	–	–
Atoms	Bond angle (°)	Atoms	Bond angle (°)	Atoms	Bond angle (°)	Atoms	Bond angle (°)
C12-O1-C26	118.3838	O1-C12-C10	125.1577	O4-C19-C23	123.0532	O1-C26-H44	105.3653
C13-O2-C27	118.4877	O1-C12-C18	114.5251	C13-C19-C23	119.6330	H42-C26-H43	109.5694
C18-O3-H40	119.1016	C10-C12-C18	120.3171	O5-C20-C9	119.7348	H42-C26-H44	109.7108
C19-O4-H41	111.1500	O2-C13-C11	124.8499	O5-C20-C24	123.1497	H43-C26-H44	109.7148
C10-C7-C14	118.1026	O2-C13-C19	115.9248	C9-C20-C24	117.0900	O2-C27-H45	111.3126
C10-C7-C16	118.3922	C11-C13-C19	119.2253	O6-C21-C9	120.0336	O2-C27-H46	111.3014
C14-C7-C16	123.5052	C7-C14-C22	120.8117	O6-C21-C25	123.4892	O2-C27-H47	104.9485
C11-C8-C15	118.2980	C7-C14-H32	120.0354	C9-C21-C25	116.4739	H45-C27-H46	109.6203
C11-C8-C17	118.4461	C22-C14-H32	119.1528	C14-C22-C18	120.9043	H45-C27-H47	109.7725
C15-C8-C17	123.2559	C8-C15-C23	120.324	C14-C22-H36	121.2131	H46-C27-H47	109.7897
C20-C9-C21	111.9152	C8-C15-H33	120.3333	C18-C22-H36	117.8825	C26-H44-H54	117.3863
C20-C9-H28	107.4837	C23-C15-H33	119.3423	C15-C23-C19	120.9334	C51-N48-H52	117.6445
C20-C9-H29	111.5877	C7-C16-C24	128.3098	C15-C23-H37	119.8702	C51-N48-H53	120.0935
C21-C9-H28	108.6115	C7-C16-H34	116.0357	C19-C23-H37	119.1963	H52-N48-H53	122.2620
C21-C9-H29	107.5570	C24-C16-H34	115.6544	C16-C24-C20	121.0522	C51-N49-H54	112.7340
H28-C9-H29	109.6432	C8-C17-C25	127.8011	C16-C24-H38	121.9135	C51-N49-C55	125.7087
C7-C10-C12	121.0536	C8-C17-H35	116.0175	C20-C24-H38	117.0341	H54-N49-C55	121.5573
C7-C10-H30	118.4855	C25-C17-H35	116.1809	C17-C25-C21	120.9780	C51-N50-H56	118.3027
C12-C10-H30	120.4609	O3-C18-C12	121.7635	C17-C25-H39	122.5274	N48-C51-N49	114.3303
C8-C11-C13	121.5861	O3-C18-C22	119.4260	C21-C25-H39	116.4944	N48-C51-N50	122.8018
C8-C11-H31	118.4324	C12-C18-C22	118.8105	O1-C26-H42	111.2116	N49-C51-N50	122.8679
C13-C11-H31	119.9814	O4-C19-C13	117.3137	O1-C26-H43	111.1871	H44-H54-N49	105.8538

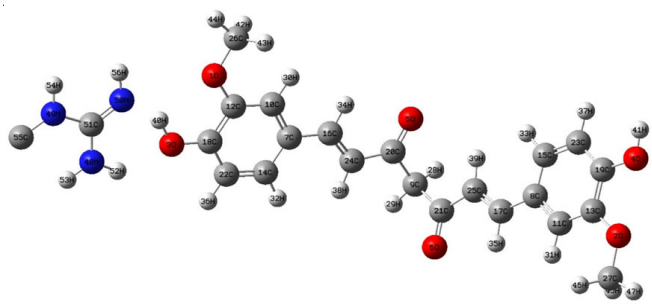

Fig. 1. Optimized guanidine-curcumin structure with numbering of atoms

of complex possesses a dual ethyl group, three nitrogen atoms and six oxygen atoms. The range of the carboxyl group (C-O) in guanidine-curcumin structure falls between 1.215 Å to 1.4515 Å and the mean C-O distance is 1.3668 Å. The distance of O3-H40 is 1.0359 Å and O4-H41 is 0.9769 Å. The average C-C-O and C-O-C bond angles is 120.378°.

The average length of C-C bond is calculated to be 1.4393 Å and the C-C average bond distance associated with six-member ring is 1.4040 Å. The mean bond angle of the C-C-C group is 120.314º. The C-H group in the complex structure possesses an average bond length of 1.086 Å, ethyl group (CH_2) consist an average C-H distance of 1.094 Å and methyl group (CH_3) exhibits a mean C-H distance of 1.0941 Å. The C-C-H group exhibited an average bond angle of 117.145º and the H-C-H possesses an average of 109.689º as bond angle. The complex structure possesses triple nitrogen atom associated to guanidine structure. It possess a centre carbon atom C51 which is attached with a triple nitrogen atom N48, N49 and N50. The nitrogen atom N49 is also attached with another carbon atom C55. The average C-N bond length is 1.3574 Å and the average N-H distance is 1.0166 Å, respectively. The C-N-H has an average bond angle of 118.066º, C-N-C has a bond angle of 125.709º and N-C-N has an average bond angle of 120º. The bond length and bond angle of the optimized guanidine-curcumin complex showed no deviation in geometry. Therefore, the accessed molecular parameters such as bond distance and angle of the complex structure were in the expected range [17,18].

Electronic spectrum: The electronic states of guanidine-curcumin complex were evaluated through theoretical UV-visible spectrum [19]. The UV-visible spectrum was computed through TD-DFT with CAM-B3LYP in the 6-311++G (d,p) theory level. Fig. 2 depicts the theoretically evaluated electronic (UV) spectrum. The excitation energy (cm^{-1}) from the TD-DFT simulation was 28697.4 cm^{-1} for 348 nm and 35808.8 cm^{-1} for 279 nm and the oscillator strength (f) for the wavelength 348 nm is 0.0011 and for wavelength 279 nm is 0.0004, respectively. The contribution of the major peak 348 nm is H→L+1 (57%), H→L+2 (27%), H-1→L+1 (2%), H→L+3 (9%) and for minor peak 279 nm, it was observed as H-1→L+1 (12%), H-1→L+2 (24%), H→L+2 (33%), H-3→L+2 (4%), H-2→L+2 (4%) and H→L+3 (4%). The transition observed for the guanidine-curcumin complex was π→π*.

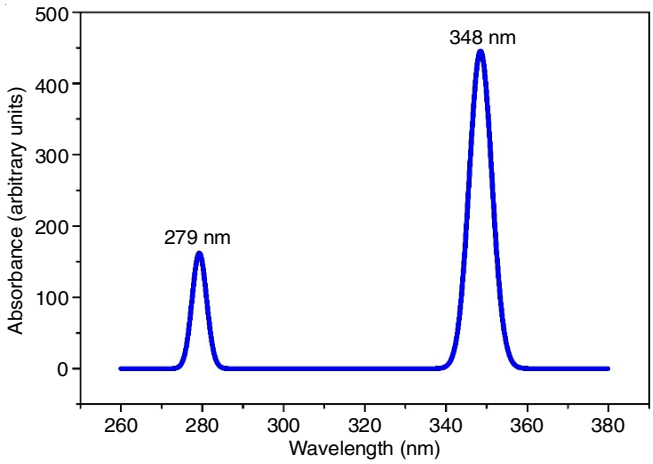

Fig. 2. Theoretically simulated UV-visible spectra of guanidine-curcumin complex

Frontier molecular orbitals (FMOs): A lower energy gapped molecule is expected to be softer, more polarizable and have a high degree of chemical hardness, although a molecule with a larger energy gap should be more stable and have a high level of chemical hardness [20]. As reported by the Koopmans' theory and the HOMO and LUMO values of the guanidine-curcumin complex, the global reactivity descriptors electron affinity (A), ionization potential (I), chemical potential (μ), electronegativity (χ), softness (S), global hardness (η) and the electrophilicity index (ω) may be calculated. Fig. 3 illustrates the plot of the acquired FMOs. The E_{LUMO}, E_{HOMO} and the estimated energy gap for the guanidine-curcumin complex was found to be calculated to be -1.97337 eV, -5.4330 eV and 3.45963 eV, respectively. Table-2 displays the entire set of data, while Fig. 4 displays the HOMO-LUMO energy map. According to the Koopmans' theorem, the electron affinity (A) and ionization potential (I), where $A = -E_{LUMO} = 1.97337$ eV and $I = -E_{HOMO} = 5.4330$ eV, respectively, are the negative energies of HOMO and LUMO, the electronegativity (χ) formula is equal to $(I + A)/2 = 3.70318$ eV. Chemical potential (μ) is the inverse of electronegativity (χ) and is computed as (χ) = -3.70318 eV from the I and A values. The chemical hardness (η) of the guanidine-curcumin complex has a value of 1.72981 eV. When $= 1/\eta = 0.57809$ eV is used to calculate chemical softness (S), the title compound is more chemically stable. The electrophilicity index, which measures the number of electrons transferred from the donor (HOMO) to the acceptor (LUMO), reduces energy. For the guanidine-curcumin complex, the nucleophilicity (N) is 0.25227 eV, while the electrophilicity (ω) is 3.96388 eV. The computed band gap energy or ΔE value, for the guanidine-curcumin complex molecule was 3.45963 eV, indicating that the molecule is stable and possesses an ΔE value equivalent to bioactive compounds. The lower electron affinity value indicates more molecular reactivity with nucleophiles (1.97337 eV). The molecule's increased molecular hardness is substantiated by higher hardness and lower softness values. Because of its negative chemical potential, the guanidine-curcumin complex is a stable molecule that is essential for biological activity. The

TABLE-2
GUANIDINE-CURCUMIN COMPLEX'S FMOs AND ASSOCIATED MOLECULAR PROPERTIES VALUES

Parameters	B3LYP/6-311++G(d,p) (eV)
E_{LUMO}	-1.97337
E_{HOMO}	-5.4330
ΔE ($E_{LUMO} - E_{HOMO}$)	3.45963
Electron affinity (A)	1.97337
Ionization potential (I)	5.4330
Chemical hardness (η)	1.72981
Chemical softness (S)	0.57809
Electronegativity (χ)	3.70318
Chemical potential (?)	-3.70388
Electrophilicity index (ω)	3.96388
Nucleophilicity index (N)	0.25227

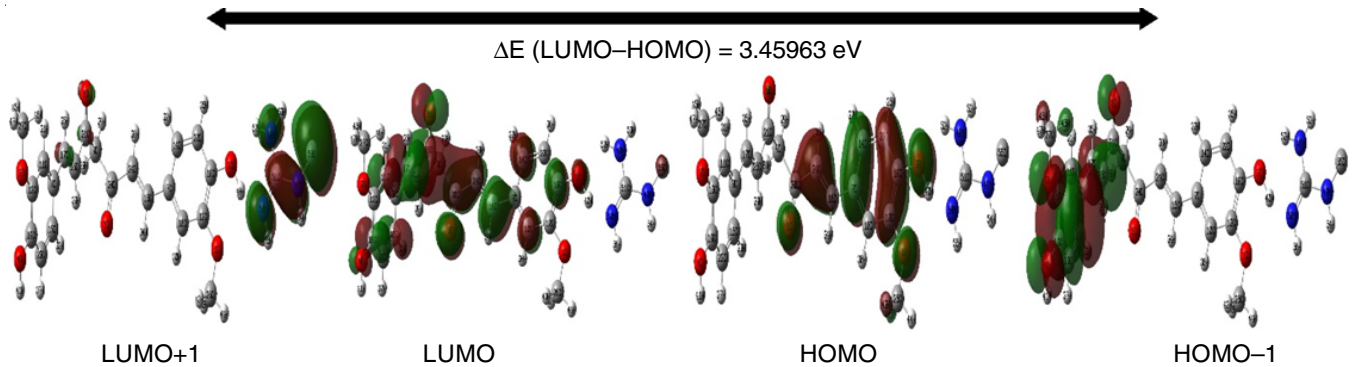

Fig. 3. HOMO, LUMO, HOMO-1, LUMO+1 orbitals of guanidine-curcumin complex

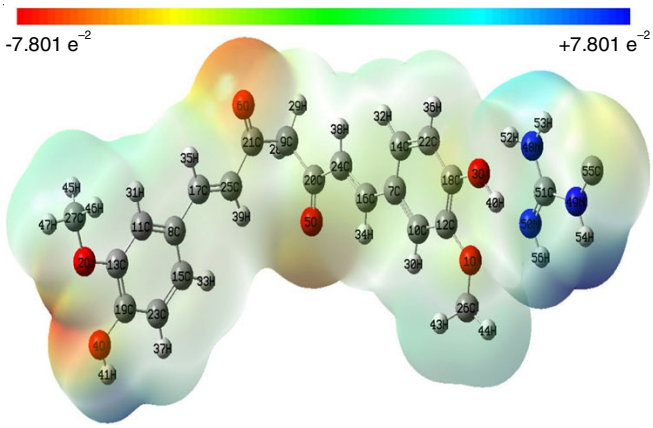

Fig. 4. Guanidine-curcumin complex's molecular electrostatic potential map

chemical's nucleophilicity and electrophilicity indices are also linked to its biological activity. The nucleophilicity index of a molecule rises as its reactivity rises.

Mulliken charge analysis: The electronic assembly, polarizability and dipole moment of guanidine-curcumin complex were determined by the mulliken atomic charge analysis [21]. The guanidine-curcumin's mulliken charges were assessed through DFT computation on B3LYP/6-311++G (d,p) level. Table-3 represents the mulliken atomic charges of each atom associated to the guanidine-curcumin complex. In this complex structure, except O1 and O6 other oxygen atoms possesses positive charges. O1 exhibited a mulliken charge of -0.03002 e and O6 has a mulliken charge of -0.01285, whereas the mulliken charge of remaining oxygen atoms lies between 0.019654 e to 0.137468 e.

The hydrogen atoms H28 to H47, H52 to H54 and H56 all possesses positive charges in the guanidine-curcumin structure. The highest positive charge was assessed for H52 atom with charge value of 0.276186 e and the lowest positive value was observed for H35 atom with charge of 0.01252 e. When it comes to carbon atoms, ten of the carbon atoms exhibits positive charge and twelve of the carbon atoms exhibits negative charges. The positive charge of the carbon atoms falls between the range of 0.002946 e to 0.388475 e and the negative charge ranges from -0.04314 e to -0.50787 e. In the three nitrogen atoms, N48 (-0.39229 e) and N50 (-0.00474 e) possesses negative charges and N49 (0.290751 e) exhibits positive charge. In guanidine-curcumin complex, the charge delocalization was observed [22].

Molecular electrostatic potential (MEP): For the constructed guanidine-curcumin complex the MEP was computed through B3LYP/6-311++G (d,p) basis set. Fig. 4 represents the surface of molecular electrostatic potential over guanidine-curcumin complex. The range of colour codes over the guanidine-curcumin complex were from -7.801 e-2 to +7.801 e-2.

The highest negative potential section (red) was observed above the all the oxygen atoms expect O1 and O3 in the guanidine-curcumin complex, whereas in O1 and O3 a slight negative potential is witnessed. Therefore, the electrophilic outbreak can be liable to the CO and CHO groups of the complex structure. The triple nitrogen atoms in the complex showed potential, by overlying of blue colour over the atoms. Most of the hydrogen and carbon atoms were witnessed to be laid in the region of blue colour. The green zone indicates the average of both positive and negative potential of the complex structure.

Molecular docking analysis: The optimized guanidine-curcumin complex was exposed to a molecular docking simulation to demonstrate the greatest inhibitory impact through protein-ligand interaction studies. The 3D crystallographic structures of the target proteins were saved from the protein data bank (PDB database) and the proteins that were saved were further processed. The proteins were processed using the Discovery Studio tool, which removed all water molecules and hetatms. The protein structures that resulted were then used in the docking process. The PyRx programme was utilized for molecular docking. The guanidine-curcumin complex was linked to certain breast cancer target proteins. The CASTp online programme was used to locate the active locations of breast cancer proteins [23]. The grid box was built with the stated areas and docking was done on the optimal active regions. Tamoxifen was chosen as a model for molecular docking studies on breast cancer-related proteins since it has previously been shown to prevent carcinoma growth [24].

Tamoxifen, a commonly used breast cancer drug, attaches to breast cancer protein receptors to limit excessive cell growth. As a result, seven target breast cancer proteins were employed

TABLE-3
MULLIKEN ATOMIC CHARGES OF GUANIDINE-CURCUMIN COMPLEX STRUCTURE

Atoms	Mulliken charges (e)	Atoms	Mulliken charges (e)	Atoms	Mulliken charges (e)	Atoms	Mulliken charges (e)
O1	-0.03002	C15	0.034565	H29	0.10958	H43	0.088191
O2	0.137468	C16	-0.32812	H30	0.019339	H44	0.058179
O3	0.019654	C17	-0.24881	H31	0.020473	H45	0.053426
O4	0.022504	C18	-0.50787	H32	0.038869	H46	0.0528
O5	0.020148	C19	-0.39864	H33	0.06049	H47	0.083977
O6	-0.01285	C20	-0.41661	H34	0.026497	N48	-0.39229
C7	0.388475	C21	-0.435	H35	0.01252	N49	0.290751
C8	0.37396	C22	0.165488	H36	0.062744	N50	-0.00474
C9	0.22982	C23	0.213791	H37	0.061246	C51	-0.2306
C10	-0.09869	C24	0.200057	H38	0.071829	H52	0.276186
C11	-0.17906	C25	0.20708	H39	0.046138	H53	0.25248
C12	-0.10642	C26	-0.04314	H40	0.230175	H54	0.189794
C13	-0.26825	C27	0.002946	H41	0.250843	C55	-0.49082
C14	0.039133	H28	0.084627	H42	0.076335	H56	0.144056

in present docking study, with tamoxifen docked in the active site locations. When compared to the other breast cancer proteins, tamoxifen's docking scores varied from -5.5 kcal/mol to -7.8 kcal/mol, with the receptor protein PR receiving the highest docking value of -7.8 kcal/mol. The docking scores for the target proteins for the main chemical, guanidine-curcumin complex, range from -7.6 kcal/mol to -10.0 kcal/mol. Guanidine-curcumin complex showed the highest binding affinity, with a docking score of -10.0 kcal/mol against the receptor protein BCL2 and a lowest docking value of -7.6 kcal/mol against two target proteins, ER-alpha and EGFR. The binding affinities of guanidine-curcumin complex and the commonly used medication tamoxifen for the target proteins are summarized in Table-4.

TABLE-4
DETAIL OF DOCKING SCORES OF GUANIDINE-CURCUMIN COMPLEX AND STANDARD DRUG

PDB ID	Proteins	Binding affinity (Kcal/mol)	
		Tamoxifen	Complex
4AQ3	BCL2	-7.7	-10.0
6WOK	ERα	-6.9	-7.6
4OAR	PR	-7.8	-7.7
2IOK	HER-2	-7.1	-7.9
4MHE	CCL 18	-6.7	-8.0
2VCJ	HSP90	-5.5	-8.9
2J6M	EGFR	-7.1	-7.6

The title chemical demonstrated a binding affinity for the target protein PR of -10.0 kcal/mol, compared to -7.7 kcal/mol for the commonly used drug tamoxifen. When compared to the BCL2 binding score discrepancies between the common medicine and the guanidine-curcumin complex, target protein PR docking scores suggest that tamoxifen (-7.8 kcal/mol) is somewhat higher than the guanidine-curcumin complex (-7.7 kcal/mol). The guanidine-curcumin complex has binding affinities of -8.9 kcal/mol for the target proteins HSP90 and CCL18, respectively. As compared to tamoxifen, guanidine-curcumin complex demonstrated good docking scores and excellent binding to breast cancer-associated proteins. As a consequence, by acting as an inhibitor of these seven key proteins, guanidine-curcumin complex structure may be used to prevent breast cancer. The docking results of guanidine-curcumin complex with the target proteins revealed a strong attraction to breast cancer proteins and the possibility for regulating these receptor proteins to limit the progression of metastatic breast cancer [25].

Interactions of protein-ligand: After the molecular docking simulation, the amino acid interactions should be analyzed for the assessment of type of bond interactions and bond distances between the receptor protein and ligand through the software tool BIOVIA discovery studio [26]. The interactions of the guanidine-curcumin complex with several target proteins associated to breast cancer are depicted in Fig. 5. The guanidine-curcumin complex and BCL2 established three (3) conventional hydrogen bonds, two (2) carbon hydrogen bonds with amino residues TYR16, ALA59, ALA108, GLY104 and PHE71 at the bond distances (Å) of 2.7338, 1.99604, 2.30643, 2.7075 and 2.91439 respectively and also established one (1) pi-pi stacked, two (2) pi-pi-T-shaped, one (1) alkyl and two (2) pi-alkyl hydro phobic interactions with amino residues TYR161, PHE63, TYR67, VAL107 and TYR161 (2) at bond distances (Å) of 3.88455, 5.43337, 4.88816, 4.4618, 4.96228 and 5.04635. The target protein CCL18 and the ligand guanidine-curcumin complex produced seven (7) conventional hydrogen bonds, three (3) carbon hydrogen bonds with amino residues TYR15, SER17, LEU13, THR31, SER32, GLU30, TYR15, VAL14, SER17 and TYR15 at bond distances (Å) of 2.43192, 2.22897, 2.45816, 1.96571, 2.37547, 2.56541, 2.07138, 2.57958, 2.91486 and 2.53195, respectively and also produced one (1) attractive charge and one (1) pi-cation electrostatic interactions with amino residues GLU30 and LYS56 at bond distances (Å) of 5.22827 and 4.58702, respectively and also established one (1) pi-pi stacked, two (2) alkyl and one (1) pi-alkyl hydro-phobic interactions with amino acids TYR15, PRO33, VAL14 and PRO33 at bond distances (Å) of 4.98968, 3.96678, 4.15096 and 4.3729, respectively.

Guanidine-curcumin complex and EGFR established one (1) conventional hydrogen bonds and three (3) carbon hydrogen bonds with amino residues ASP855 (2), ARG841 and ASP800 at bond distances (Å) of 2.58162, 2.65245, 2.6869 and 2.90288 respectively and also produced attractive charge electrostatic interaction with amino residue ASP800 at the bond distance (Å) of 5.46803 and also established two (2) alkyl and three (3) pi-alkyl hydrophobic bond interactions with amino acids LEU718, VAL726 (2), ALA743 and LEU844 at bond distances (Å) of 4.6567, 3.66327, 4.95534, 4.03416 and 4.79369, respectively. Guanidine-curcumin complex with an ERα receptor protein established one (1) conventional hydrogen bonds, four (4) carbon hydrogen bonds with amino residues SER372 (3) and ASP374 (2) at bond distances (Å) of 2.41726, 2.87617, 2.95553, 2.89681 and 2.90952, respectively and also produced one (1) attractive charge electrostatic interaction with amino residue ASP374 at the bond distance (Å) of 5.3611 and also established one (1) alkyl and three (3) pi-alkyl hydrophobic interactions with amino residues LEU541, HIS373 and LEU541 (2) at bond distances (Å) of 4.07688, 4.49242, 4.38335 and 5.32888, respectively. The target protein HER2 and guanidine-curcumin complex produced one (1) conventional hydrogen bond and four (4) carbon hydrogen bond interactions with amino residue GLU1353, GLY1521 (2) and LEU 1346 (2) at bond distances of 2.63274, 2.6605, 2.76062, 3.09298 and 2.83826 and also produced one (1) pi-sulfur interaction with amino residue MET1343 at the bond distance (Å) of 4.83331 and also established one (1) pi-sigma, one (1) pi-pi T-shaped, three (3) alkyl and four (4) pi-alkyl hydrophobic interactions with amino residues LEU1525, PHE1404, ALA1350, LEU-1346, LEU1349, LEU1346, ALA1350, LEU1387, MET1388 and LEU1391 at bond distances (Å) of 2.48112, 5.43971, 3.78373, 5.04271, 4.44431, 4.36019, 5.44166, 4.44874, 5.48764 and 4.93795, respectively. HSP90 with guanidine-curcumin complex formed two (2) conventional hydrogen bonds and one (1) carbon hydrogen bond interactions with amino residues ASN51, GLY132 and ASP54 at bond distances (Å) of 2.11753, 2.92561, 2.92561 and 2.58853 respectively and also produced one (1) attractive charge and one (1) pi-anion electrostatic interactions with amino residue ASP54 (2) at bond distances (Å)

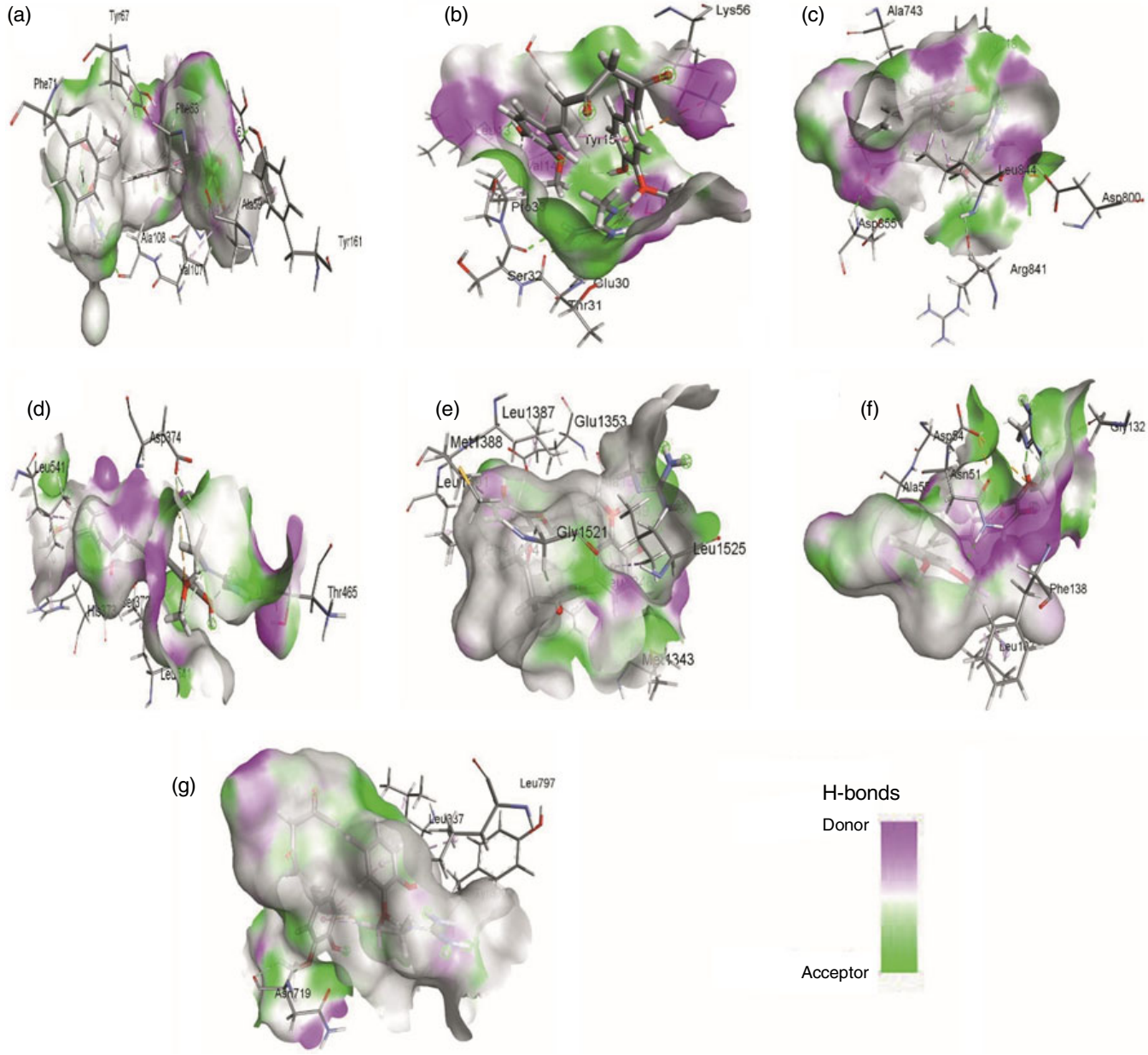

Fig. 5. 3D interactions of guanidine-curcumin complex with (a) BCL2 (b) CCL18 (c) EGFR (d) ERα (e) HER-2 (f) HSP90 and (g) PR target proteins

of 4.69406 and 4.97023 respectively and also established one (1) alkyl and two (2) pi-alkyl hydrophobic bond interactions with amino residues LEU107, PHE138 and ALA55 at bond distances (Å) of 4.02087, 4.72343 and 5.03017, respectively. The title guanidine-curcumin complex with PR formed one (1) conventional hydrogen bonds and two (2) carbon hydrogen bond interactions with amino residues TYR890 and ASN719 (2) at bond distances of 2.98679, 2.69701 and 2.76404, respectively and also established two (2) Pi-Alkyl hydrophobic bond interactions with amino residues LEU797 and LEU887 at bond distances of 4.8194 and 5.00835, respectively.

There are produced various types of amino acid interactions in between breast cancer associated proteins and guanidine-curcumin complex such as hydrogen bond interactions, hydrophobic interactions and electrostatic interactions [27]. From the CASTp study, the guanidine-curcumin complex was excellently interacted with the seven target proteins at the predicted active site of the targeted receptor proteins. According to the amino acid interactions between guanidine-curcumin complex and breast cancer relevant proteins, the guanidine-curcumin complex produces excellent interactions with various amino residues of the above-mentioned receptor proteins, guanidine-curcumin complex may be an achievable therapy for breast cancer.

Pharmacokinetic prediction: The ADME/Tox profile describes a drug's absorption (A), distribution (D), metabolism (M), excretion (E) and toxicity (Tox). This *in silico* pharmacokinetics assessment is a useful online tool for predicting the ADME and hazardous characteristics of drug candidates under investigation, particularly at the preclinical level [28]. The

computerized and *in silico* models have been developed to generate accurate pharmacokinetic and toxicological predictions. The pre-programmed models are beneficial for drug development and preventing early elimination of drug candidate; hence, they save significant amounts of non-productive time and money. In this *in silico* study, two relatively new web tools were employed; the cost-effective SwissADME web tool, which is a current and pertinent web server to predict the physicochemical characteristics of the compounds and free pkCSM-pharmacokinetics web tool, which is utilized to investigate the ADMET characteristics of the compounds. The optimized guanidine-curcumin complex structure was represented in SMILES (simplified molecular input line-entry standard) for usage in the online tools, SwissADME and pkCSM-pharmacokinetics. According to the Swiss ADME, guanidine-curcumin complex does not affect Lipinski's rules, so the guanidine-curcumin complex can be taken as oral medication. Lipophilicity, aqueous solubility and the percentage level of human intestinal absorption qualities were used to assess estimated absorption. The researched guanidine-curcumin complex is thought to have low GI absorption. Moreover, drug bioavailability was connected to TPSA (topological polar surface area); if a molecule's TPSA is ≤ 140 Å^2, this GuC complex would have an estimated somewhat good bioavailability with a value of 154.96 Å^2, supporting the possibility of projected passive oral absorption. The water solubility of the guanidine-curcumin complex was -3.68, indicating that it is only marginally soluble in water. The lipophilicity value was calculated *via* the logarithm of the *n*-octanol/water partition coefficient, which was assessed through SwissADME's consensus LogPo/w parameter. LogPo/w is significantly associated with transport processes linking human membrane permeability and circulation to various organs and tissues. In general, for a chemical to have appropriate oral bioavailability in humans, it should have a moderate logP ($0 < \log P < 3$) [29]. The calculated value of logPo/w for guanidine-curcumin complex was 2.47, confirming the complex's strong lipophilicity. The pkCSM-pharmacokinetic properties were used to determine the proportion of intestinal absorption in people to support the SwissADME estimates. According to the pkCSM-pharmacokinetics, the investigated guanidine-curcumin complex has an intestine absorption percentage of 64.54%. SwissADME was used to estimate distribution and blood-brain barrier (BBB) (Fig. 6) penetration, while pkCSM-pharmacokinetics was used to determine percent unbound parameters. The guanidine-curcumin complex did not pass across the BBB; it is not a substrate for the P-gp efflux pump and it does not have an inhibitory mechanism against P-gp I and II. As a result, they have no ability to cross the BBB and are expected to have no CNS adverse effects.

Proper equilibrium exists between the unbound and bound states of albumin and other serum proteins. The unbound fraction of the guanidine-curcumin complex bound to serum proteins in plasma influences hepatic biotransformation and renal glomerular excretion, influencing total drug clearance, volume of distribution and efficacy. The more the drug's plasma protein binds in the blood, the worse effectively it can disperse across cell membranes [30]. The unbound fraction value for guanidine-curcumin complex in human plasma is calculated to be 0.188 Fu in this study. The pkCSM server was utilized to forecast the metabolism of the investigated compound by evaluating the ability of these molecules to block the key cytochrome (CYP 450) enzymes and its isoforms such as CYP1A2, CYP2C19, CYP2C9, CYP2D6 and CYP3A4. Because CYP enzymes are one of the most essential enzymes involved in the body's xenobiotic metabolism, especially oxidation. Inhibiting these enzymes may result in the drug-drug interactions related to metabolism, often including competing for the same enzyme binding site with another co-administered medication. Inhibition of this cytochrome 450 enzymes may affect the metabolism and clearance of further co-administered xenobiotics, resulting in higher plasma levels of these medications, which alter their therapeutic efficacy. Consequently, CYP inhibition can degrade and cause xenobiotic toxicity or, at the very least, a loss of a drug's therapeutic advantages. Moreover, the examined guanidine-curcumin complex does not function as a substrate for CYP isoforms and does not inhibit any of them except CYP3A4. Notably, guanidine-curcumin complex has the least efficacy as a cytochrome P450 enzyme inhibitor. Excretion is a pharmacokinetic parameter that combines hepatic and renal excretion, is related to bioavailability and is crucial for setting dosages at rates to achieve steady-state concentrations for specific medications. The overall clearance and renal OCT2 substrate parameters were calculated *via* the pkCSM pharmacokinetics online server to estimate excretion. To begin, guanidine-curcumin complex had a total clearance value of 1.01 (log mL/min/kg).

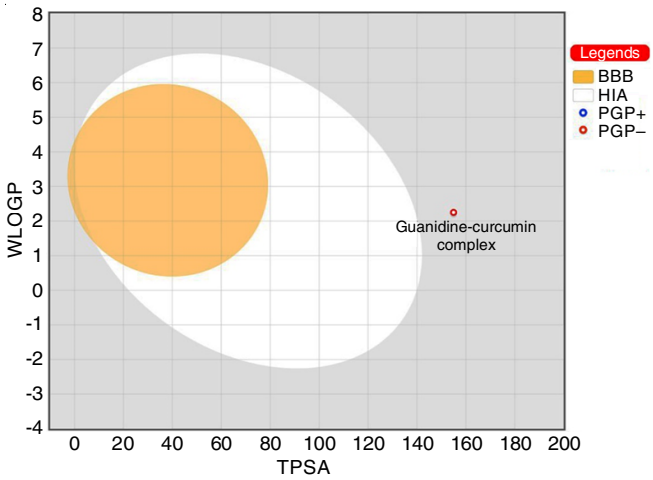

Fig. 6. Predicted boiled-egg model of guanidine-curcumin complex

As shown in Table-5, the examined guanidine-curcumin complex is not a predicted substrate for renal OCT2 transport protein. Finally, pkCSM pharmacokinetics was used to predict the hepatotoxicity and acute toxicities of examined guanidine-curcumin complex in rats. The guanidine-curcumin complex has an LD50 value of 2.03 mol/kg. The liver functions as the primary organ for drug and xenobiotic metabolism and plays an important role in energy exchanges. As a result, a damaged liver will disrupt normal biotransformation and may potentially end in cirrhosis and liver failure. According to the hepatotoxicity criterion, the investigated guanidine-curcumin complex does not produce hepatotoxicity [31]. From the above physico-

TABLE-5
PREDICTED PHARMACOKINETIC CHARACTERISTICS OF THE GUANIDINE-CURCUMIN COMPLEX

Properties	Descriptors	Value
Physico-chemical properties	Formula	$C_{23}H_{27}N_3O_6$
	Molecular weight (g/mol)	441.48
	Number of heavy atoms	32
	Number of aromatic heavy atoms	12
	Fraction Csp3	0.17
	Number of rotatable bonds	9
	Number of H-bond acceptors	7
	Number of H-bond donors	5
	Molar Refractivity	123.63
	TPSA (Å2)	154.96
	Log Po/w (iLOGP)	3.13
	Log Po/w (XLOGP3)	2.26
	Log Po/w (WLOGP)	2.25
	Log Po/w (MLOGP)	0.69
	Log Po/w (SILICOS-IT)	4.04
	Consensus (log Po/w)	2.47
	Bioavailability score	0.55
Absorption	Water solubility (log mol/L)	-3.341
	Caco2 permeability (log Papp in 10^{-6} cm/s)	-0.282
	Human intestinal absorption (% absorbed)	64.54
	Skin permeability (log Kp)	-2.735
	P-glycoprotein substrate	Yes
	P-glycoprotein I/II inhibitors	No
Distribution	VDss (human) (log L/kg)	0.417
	BBB permeability (log BB)	0.188
	CNS permeability (log PS)	-3.435
Metabolism	CYP2D6 substrate	No
	CYP3A4 substrate	No
	CYP1A2 inhibitor	No
	CYP2C19 inhibitor	No
	CYP2C9 inhibitor	No
	CYP2D6 inhibitor	No
	CYP3A4 inhibitor	Yes
Excretion	Total clearance (log mg/kg/day)	1.01
	Renal OCT2 substrate	No
Toxicity	AMES toxicity	No
	Max. tolerated dose (human) (log mg/kg/day)	-0.124
	Oral rat acute toxicity (LD_{50}) (mol/kg)	2.030
	Oral rat chronic toxicity (LOAEL) (log mg/kg_bw/day)	2.826
	Hepatotoxicity	No

chemical and pharmacokinetic properties, it was revealed that the chemical guanidine-curcumin complex has excellent bioavailability and drug-like properties.

Conclusion

The complex structure of guanidine-curcumin was built through ChemDraw Pro and the structure was optimized through DFT with B3LYP/6-311++G (d,p) and the values for structural qualities including bond length and bond angle were calculated. The examination of the theoretical UV-visible spectra reveals an electronic transition from π to π*. According to molecular orbital assessment, the complex structure's molecular reactivity, kinetic stability and intramolecular charge transfer are all fundamentals that affect the bioactivity of guanidine-curcumin complex. Electrostatic potential surface of guanidine-curcumin assists as an accompanying verification of its reactive site. The responsive spot of the complex structure was recognized by means of the mulliken atomic charge distribution study. The *in silico* molecular docking simulation was computed through PyRx tool and the docking scores of complex structure against breast tumor targets falls between -7.6 to -10 Kcal/mol, which confirms guanidine-curcumin's breast cancer repressive latent when compared to standard drug. The drug safety assessment was predicted through theoretical estimation of the physico-chemical and ADMET properties and guanidine-curcumin complex revealed no violation in the rules.

ACKNOWLEDGEMENTS

The authors acknowledge Dr. S. Athimoolam, Department of Physics, University college of Engineering, Anna University, Nagercoil, India for helping in utilizing Gaussian program.

CONFLICT OF INTEREST

The authors declare that there is no conflict of interests regarding the publication of this article.

REFERENCES

1. R.L. Siegel, K.D. Miller and A. Jemal, *CA Cancer J. Clin.*, **69**, 7 (2019); https://doi.org/10.3322/caac.21551
2. N. Arunadevi, M. Swathika, B.P. Devi, P. Kanchana, S.S. Sundari, S.J. Kirubavathy, P. Subhapriya and E.R. Kumar, *Surf. Interfaces*, **24**, 101094 (2021); https://doi.org/10.1016/j.surfin.2021.101094
3. A. Allegra, V. Innao, S. Russo, D. Gerace, A. Alonci and C. Musolino, *Cancer Invest.*, **35**, 1 (2017); https://doi.org/10.1080/07357907.2016.1247166
4. Z.Y. Wang and L. Yin, *Mol. Cell. Endocrinol.*, **418**, 193 (2015); https://doi.org/10.1016/j.mce.2015.04.017
5. J. Kiani, A. Khan, H. Khawar, F. Shuaib and S. Pervez, *Pathol. Oncol. Res.*, **12**, 223 (2006); https://doi.org/10.1007/BF02893416
6. T.M. Viswanathan, K. Chitradevi, A. Zochedh, R. Vijayabhaskar, S. Sukumaran, S. Kunjiappan, N.S. Kumar, K. Sundar, E. Babkiewicz, P. Maszczyk and T. Kathiresan, *Cancers*, **14**, 3490 (2022); https://doi.org/10.3390/cancers14143490
7. G. Palma, G. Frasci, A. Chirico, E. Esposito, C. Siani, C. Saturnino, C. Arra, G. Ciliberto, A. Giordano and M. D'Aiuto, *Oncotarget*, **6**, 26560 (2015); https://doi.org/10.18632/oncotarget.5306
8. J. Chen, Y. Yao, C. Gong, F. Yu, S. Su, J. Chen, B. Liu, H. Deng, F. Wang, L. Lin, H. Yao, F. Su, K.S. Anderson, Q. Liu, M.E. Ewen, X. Yao and E. Song, *Cancer Cell*, **19**, 541 (2011); https://doi.org/10.1016/j.ccr.2011.02.006
9. N.I. Ziedan, R. Hamdy, A. Cavaliere, M. Kourti, F. Prencipe, A. Brancale, A.T. Jones and A.D. Westwell, *Chem. Biol. Drug Des.*, **90**, 147 (2017); https://doi.org/10.1111/cbdd.12936
10. I. Koca, A. Özgür, M. Er, M. Gümüs, K. Açikalin Coskun and Y. Tutar, *Eur. J. Med. Chem.*, **122**, 280 (2016); https://doi.org/10.1016/j.ejmech.2016.06.032
11. M.E. Vaschetto, B.A. Retamal and A.P. Monkman, *J. Mol. Struct. THEOCHEM*, **468**, 209 (1999); https://doi.org/10.1016/S0166-1280(98)00624-1
12. A. Zochedh, A. Shunmuganarayanan and A.B. Sultan, *J. Mol. Struct.*, **1274**, 134402 (2023); https://doi.org/10.1016/j.molstruc.2022.134402
13. S. Thangarasu, A. Chitradevi, V. Siva, A. Shameem, A. Murugan, T.M. Viswanathan, S. Athimoolam and S.A. Bahadur, *Polycycl. Aromat. Compds.*, (2022); https://doi.org/10.1080/10406638.2022.2064883

14. A. Kouranov, L. Xie, J. de la Cruz, L. Chen, J. Westbrook, P.E. Bourne and H.M. Berman, *Nucleic Acids Res.*, **34(suppl_1)**, D302 (2006); https://doi.org/10.1093/nar/gkj120
15. S. Dallakyan and A.J. Olson, *Methods Mol. Biol*., **1263**, 243 (2015); https://doi.org/10.1007/978-1-4939-2269-7_19
16. K. Al-Azzam, *Kompleksnoe Ispolzovanie Mineralnogo Syra*, **325**, 14 (2023); https://doi.org/10.31643/2023/6445.13
17. T.M. Kolev, E.A. Velcheva, B.A. Stamboliyska and M. Spiteller, *Int. J. Quantum Chem.*, **102**, 1069 (2005); https://doi.org/10.1002/qua.20469
18. V. Siva, S.S. Kumar, A. Shameem, M. Raja, S. Athimoolam and S.A. Bahadur, *J. Mater. Sci. Mater. Electron.*, **28**, 12484 (2017); https://doi.org/10.1007/s10854-017-7070-8
19. S. Sukumaran, A. Zochedh, T.M. Viswanathan, A.B. Sultan and T. Kathiresan, *Polycycl. Arom. Compounds*, (2023); https://doi.org/10.1080/10406638.2022.2164018
20. M. Priya, A. Zochedh, K. Arumugam and A.B. Sultan, *Chemistry Africa*, **6**, 287 (2022); https://doi.org/10.1007/s42250-022-00508-z
21. A. Zochedh, M. Priya, C. Chakaravarthy, A.B. Sultan and T. Kathiresan, *Polycycl. Arom. Compds.*, (2022); https://doi.org/10.1080/10406638.2022.2118332
22. S. Thangarasu, V. Siva, S. Kannan, S.A. Bahadur and S. Athimoolam, *Polycycl. Arom. Compds.*, (2022); https://doi.org/10.1080/10406638.2022.2130374
23. W. Tian, C. Chen, X. Lei, J. Zhao and J. Liang, *Nucleic Acids Res.*, **46(W1)**, W363 (2018); https://doi.org/10.1093/nar/gky473
24. S.G. Nayfield, J.E. Karp, L.G. Ford, F.A. Dorr and B.S. Kramer, *J. Natl. Cancer Inst.*, **83**, 1450 (1991); https://doi.org/10.1093/jnci/83.20.1450
25. A. Zochedh, K. Chandran, M. Priya, A.B. Sultan and T. Kathiresan, *J. Mol. Struct.*, **1285**, 135403 (2023); https://doi.org/10.1016/j.molstruc.2023.135403
26. LIGAND Design, Pharmacophore and Ligand-based Design with Biovia Discovery Studio®, BIOVIA, California (2014).
27. A. Zochedh, M. Priya, A. Shunmuganarayanan, A.B. Sultan and T. Kathiresan, *J. Mol. Struct.*, **1282**, 135113 (2023); https://doi.org/10.1016/j.molstruc.2023.135113
28. U. Norinder and C.A.S. Bergström. *ChemMedChem*, **1**, 920 (2006); https://doi.org/10.1002/cmdc.200600155
29. K.R. Sharmili Banu, I.M. Priya and A.S. Azar Zochedh, *Asian J. Biotechnol. Genetic Eng.*, **5**, 9 (2022).
30. K. Chandran, D.I. Shane, A. Zochedh, A.B. Sultan and T. Kathiresan, *In Silico Pharmacol.*, **10**, 14 (2022); https://doi.org/10.1007/s40203-022-00130-4
31. L.L.G. Ferreira and A.D. Andricopulo, *Drug Discov. Today*, **24**, 1157 (2019); https://doi.org/10.1016/j.drudis.2019.03.015